

Determination of mask induced polarization effects occurring in Hyper NA immersion lithography

Silvio Teuber^{1*}, Karsten Bubke¹, Ingo Höllein¹, Ralf Ziebold², Jan Hendrik Peters¹

¹Advanced Mask Technology Center GmbH & Co. KG, Raehntzer Allee 9, D-01109 Dresden, Germany

²Infineon Technologies SC300 GmbH & Co. KG, Koenigsbruecker Strasse 180, D-01079 Dresden, Germany

ABSTRACT

As the lithographic projection technology of the future will require higher numerical aperture (NA) values, new physical effects will have to be taken into consideration. Immersion lithography will result in NA values of up to 1.2 and above. New optical effects like 3D shadowing, effects from oblique incident angles, mask-induced polarization of the transmitted light and birefringence from the substrate should be considered when the masks optical performance is evaluated. This paper addresses mask induced polarization effects from dense lines-and-space structures of standard production masks. On a binary and on an attenuated phase-shifting mask, which were manufactured at the Advanced Mask Technology Center (AMTC) transmission experimental investigations were performed. Measurements of diffraction efficiencies for TE- and TM-polarized light using three different incident angles are presented for all considered mask types and compared to simulations. The structures under investigation include line-space-pattern with varying pitches as well as varying duty cycles. Experimental results show good agreement with simulations.

Keywords: Polarization, high NA, immersion lithography, binary masks, attenuated phase shift masks

1. INTRODUCTION

As reported earlier, mask induced polarization effects become a concern when smaller features need to be produced in conjunction with the usage of increasing numerical apertures [1]. The half pitch of the smallest resolved feature size is given by:

$$HP_{MIN} = \frac{\lambda}{2(\sigma + 1)NA}, \quad (1)$$

where λ is the exposure wavelength, σ is the partial coherence grade and NA is the numerical aperture. The corresponding half pitch on the mask (HP_{mask}) is multiplied by the magnification factor M . Assuming $\sigma=1$, the half pitch on the mask is given by:

$$HP_{Mask} = \frac{\lambda}{NA}, \quad (2)$$

and is in the range of the exposure wavelength.

Reticle features with half pitches $\sim \lambda/4$ can act as a polarizer ($HP_{mask} \sim 48\text{nm}$), known as Hertzian or wire grid polarizer. In this case the light going through the grating is completely TM polarized. TM polarization is defined as polarization state, in which the electric field resides in the plane of incidence. The electrical field oscillating perpendicular to the plane of incidence is referred to as TE polarization state. Figure 1 shows a description of TE & TM polarization directions.

Furthermore, reticle features with half pitches $\sim \lambda$ can also act as a partial polarizer ($HP_{mask} \sim 193\text{nm}$, corresponding to $HP_{wafer} \sim 48\text{nm}$). In this relevant case, the light propagating through the grating structure will output a mix of TE (or s) and TM (or p) polarization resulting in a partial linear polarization. The efficiency of the mask induced partial

* Phone: +49-351-4048-364, Fax: +49-351-4048-9364, E-mail: Silvio.Teuber@amtc-dresden.com

polarization is strongly influenced by the pitch, duty cycle, absorber geometry (thickness, shape, sidewall angle), and absorber material [1,5].

A series of experiments and simulations were performed in order to investigate quantitatively the mask-induced polarization for all relevant mask materials. The experimental setup is shown in Figure 1. The photomask is illuminated with either polarized or unpolarized light, resulting in different diffraction orders. An angle resolved detector measures the intensity of the transmitted light, from which one derives the degree of polarization (DoP):

$$DoP = \frac{I_{TE} - I_{TM}}{I_{TE} + I_{TM}}. \quad (3)$$

A DoP of -100% indicates a fully TM polarized radiation, whereas $+100\%$ is characteristic of fully TE polarized radiation. A DoP of 0% corresponds to equally TE and TM polarization.

At the same time rigorous coupled wave analysis simulations were performed where binary and phase shift masks with different grating periods and duty cycles were investigated.

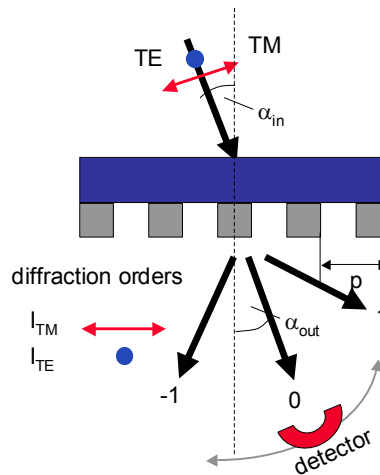


Figure 1: Experimental setup: polarized light propagates through a photomask. A detector is measuring the angle dependent intensity of the different diffraction orders.

2. DESIGN, FABRICATION and CHARACTERIZATION of GRATING RETICLES

In order to investigate the mask induced polarization effects, masks with grating structures of different periods and duty cycles were produced. The duty cycle is defined as the line size divided by the pitch size (line/pitch). To enable meaningful comparison the grating geometries manufactured on different mask types need to have well defined structure sizes, e.g. pitch size, critical dimension size (CD) and especially duty cycles (DC). Since the mask manufacturing process influences the feature sizes depending on the structure size, the finally measured CD is different compared to the designed value. This so-called process bias needs to be taken into account, when designing the mask. We applied on the mask design a data correction, which is CD and pitch dependent.

A mask design was created including the data correction described above. It consists of an array of dense lines and space gratings. The pitch size varies from 200nm-3200nm along the vertical direction, while the duty cycle changes from 0.15-0.6 (line/pitch) along the horizontal axis. The 4mm x 4mm gratings are equally distributed over the mask active field. A gap of 1mm separates the gratings (see Figure 2).

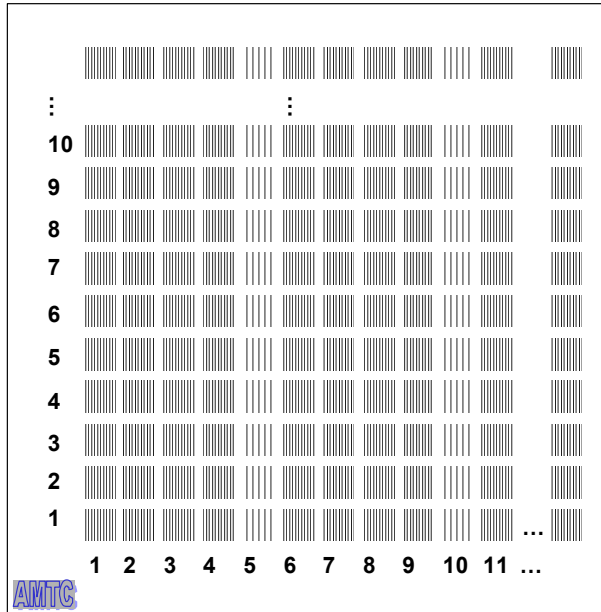


Figure 2: Principle layout of the test mask design for the polarization measurement study. Vertical dense lines and space gratings with varying pitch (in vertical direction) and varying duty cycle (in horizontal direction) are distributed over the mask.

A binary (CoG) and an attenuated phase shifting mask (AttPSM) were produced with this design at the Advanced Mask Technology Center (Dresden, Germany) using the standard manufacturing process. The mask blank materials, from Hoya, were chromium based and molybdenum silicon based (MoSi) for the CoG and AttPSM respectively. An important part in this study is the mask structure characterization, e.g. CD, sidewall angle and trench depth. We used different methods: a Holon Mask CD-SEM (secondary electron microscope) tool determines the line and space CDs, an FEI SNP (surface nano-profiler) tool and an AFM (atomic force microscope) measure the sidewall angles and trench depths (see Figure 3).

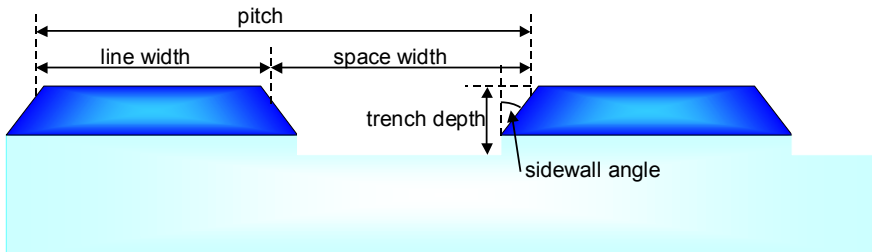


Figure 3: Schematic view of an attenuated phase shift mask grating structure

Outgoing from the CD measurement results we chose all gratings with a duty cycle = line/pitch of 0.5, e.g. 1:1 structures, as well as all gratings with a pitch of 400nm (corresponds to 50nm half pitch at wafer level). CD measurement errors of the analyzed pitch sizes of the dense lines/space patterns revealed <0.5% deviation from the design value. The determination of the duty cycle depends on the sidewall angle and on the calibration of the SEM tool. The used CD-SEM uses a calibration, in which the CD is measured at 85% of the absorber height. Taking into account that the measured sidewall angle is $>87^\circ$ for all grating structures, the measured CD deviates from the top CD only by $<1\text{nm}$. This results into the conclusion that the derived duty cycles from the CD measurements having a maximum error of about 5%.

3. EXPERIMENTAL SETUP of POLARIZATION MEASUREMENTS

The polarization measurements were performed at Fraunhofer Institute IOF in Jena using a VUV spectrophotometer (see Figure 4) [2]. The measurement system uses a deuterium lamp light source. A grating monochromator selects the specified wavelength, a Rochom prism of MgF2 determines the polarization direction and a photo multiplier measures the light intensity. Angle resolved transmission measurements were performed at 193.4nm with different polarization settings. A second photo multiplier measures the reference signal to ensure normalized intensity spectra. The rotation of the sample holder enables different incoming light incident angles from 0° to 20°. Each lines/space grating were illuminated from the backside under different polarization settings (TE-polarized, TM-polarized, unpolarized) and under different incident angles (0°, 10° and 20°). The angle resolved transmission spectra were analyzed with respect to the intensities of the 0th and the -1st diffraction order. A Gaussian-like pulse shape is fitted to the diffraction order peaks to determine the angle position and the maximum intensity. The observed angle difference 0th and -1st order can be used to verify the grating pitch:

$$pitch = \frac{\lambda}{\sin \alpha_0 - \sin \alpha_{-1}} . \quad (5)$$

The resulting intensities for the different polarization settings where used to calculate the degree of polarization (as defined in Equation 3).

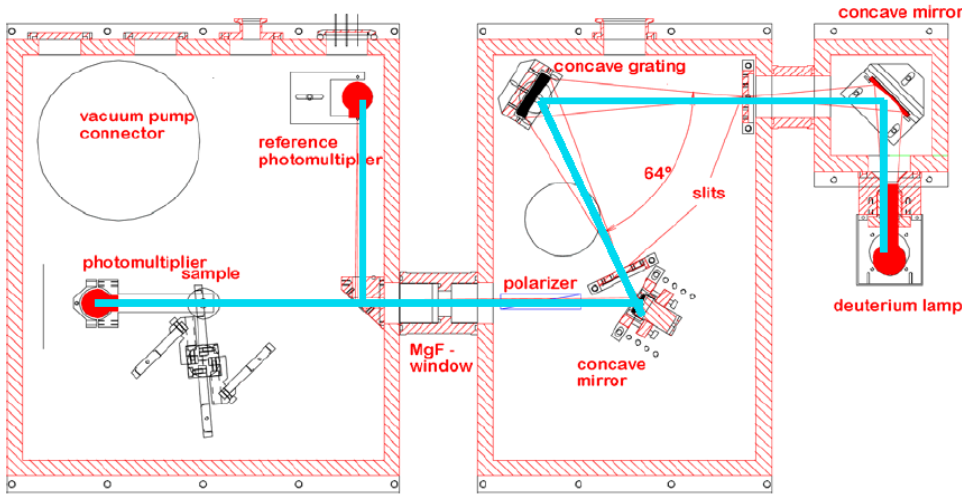
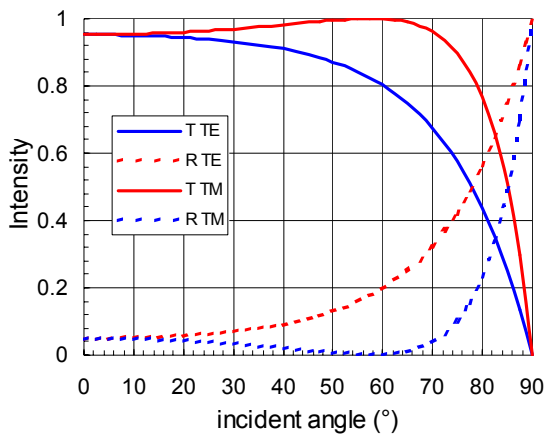


Figure 4: Schematic view of the optical system for polarization measurements done at Fraunhofer Institute IOF in Jena.

4. SIMULATIONS of MASK INDUCED POLARIZATION

Simulation was performed to understand the measurement results and to discuss their influence on imaging performance. The commercially available full 3-dimensional diffraction grating analysis tool GSOLVER (version 4.20b) [3] using hybrid rigorous coupled wave analysis and modal analysis was utilized to calculate diffraction efficiencies from plane wave illumination of dense lines and space grating structures. The same variation of the illumination settings as in the experiment was used, e.g. different incidences (0°, 10°, 20°) and different polarization settings (TE, TM). The resulting diffraction efficiencies were used for comparison to the experimental observations and to calculate the mask induced polarization.

Since the GSOLVER simulation tool is restricted to the transmission of only one surface (with the structured layer), the Fresnel reflection at the backside was added to the calculation. The results are shown on Figure 5 showing typical reflection and transmission curves. Concentrating on the angle range between 0° and 20° the light reflection is lower than 6%. Additionally, there is a small difference in the reflection of TE and TM light (see table on Figure 5). Only at the well-known Brewster angle the reflected light is fully TE-polarized resulting in none TM-reflection at ~60°.



angle	T TE (%)	T TM (%)	R TE (%)	R TM (%)	Diff (%)
0	95.2	95.2	4.79	4.79	0
10	95.0	95.4	4.98	4.68	0.38
20	94.4	96.0	5.6	4.0	1.56

Figure 5: Simulated Fresnel reflection and transmission at one quartz surface ($n_{\text{quartz}}=1.56$) at $\lambda=193\text{nm}$.

Figure 6 shows the simulated degree of polarization (DoP) of binary and attenuated-phase-shifting masks with a duty cycle of line/pitch=0.5 at normal incidence for different mask pitches (corresponds to 8^*CD at wafer level). Comparing the degree of polarization between the different mask type structures, the DoP curves for both 0^{th} and -1^{st} diffraction orders for binary mask grating runs well above that ones of the AttPSM gratings. This indicates that the AttPSM structures exhibit stronger polarization in the TM direction. The DoP for CoG of the 0^{th} order is in the negative range and of the -1^{st} order positive and negative in the whole pitch range. The DoP for AttPSM of the 0^{th} order is in the deep negative area and of the -1^{st} order also mainly negative in the whole pitch range. All DoP curves of the AttPSM structures show a strong pitch dependency, especially the polarization increases when decreasing the pitch size below 386nm . The polarization of the binary masks exhibits only in the -1^{st} diffraction order a pitch dependency. Furthermore, two significant discontinuities at $\sim 386\text{nm}$ and at $\sim 580\text{nm}$ can be observed, corresponding to Wood's Anomalies [1], where higher diffraction orders will appear. Comparing the polarization of mask features required for CDs of 50nm on wafer level, e.g. 400nm pitch mask structures, the DoP of binary masks shows a small TM polarization in 0^{th} order and a significant TE polarization in -1^{st} order. AttPSM structures induce a significant TM polarization in 0^{th} order and no polarization in -1^{st} order. The polarization values are still in the same range compared to that for higher CD sizes. But for smaller CDs the situation changes, especially at 40nm CD at wafer level, there is a strong increase of the polarization for AttPSM structures.

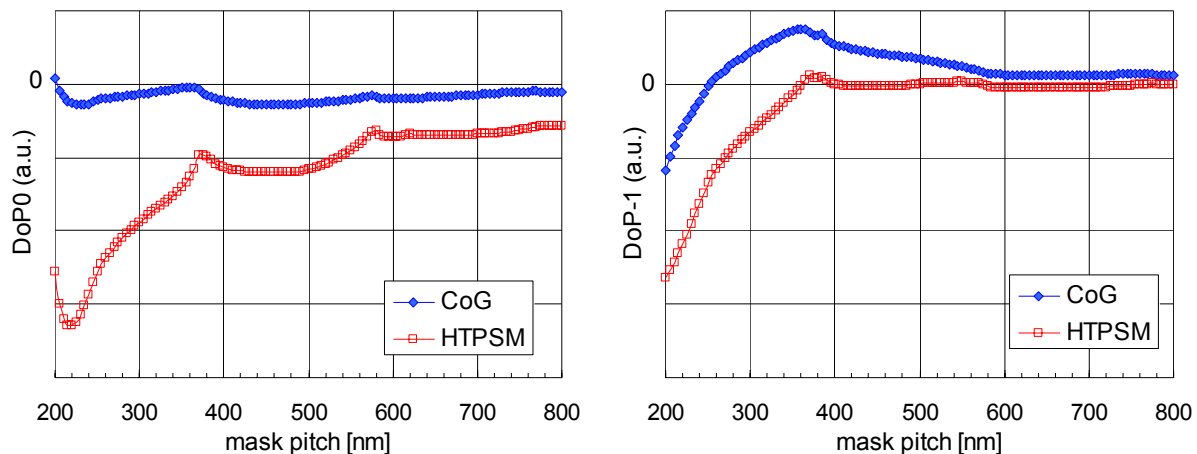


Figure 6: Simulated polarization degree of 0^{th} and -1^{st} diffraction order for 1:1 dense line space pattern illuminated with normal incidence.

Figure 7 illustrates the DoP for structures with 50nm half pitch at wafer level, e.g. dense lines/space pattern with a mask pitch=400nm and for different duty cycles. Both mask types show a small polarization in the relevant range duty cycle range 0.1-0.5. As observed in the DoP simulations depending on pitch size, the polarization curve of binary mask structures runs mainly above the curve of AttPSM structures. The DoP for CoG of the 0th order is in the positive and negative range and of the -1st order only positive in the whole duty cycle range. The DoP for AttPSM of the 0th order is only in the negative range and of the -1st order is both positive and negative in the whole duty cycle range. The strong increase of the polarization effects is due to the reduced transmission when increasing the line/pitch-ratio.

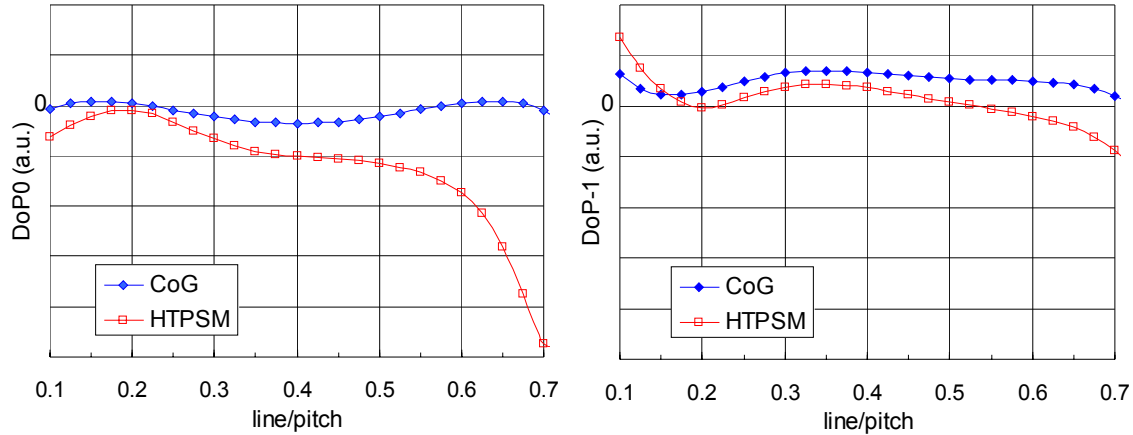


Figure 7: Simulated degree of polarization of 0th and -1st diffraction order for dense line space pattern with varying line/pitch at 400nm fixed pitch and normal incidence light settings.

The energy ratio between the transmitted, reflected and absorbed light is depicted in Figure 8 when illuminating attenuated phase shift mask structures. As described above, the TE transmission is lower than the TM resulting in partial TM polarization. Since the reflected light portion is nearly the same for TE and TM the absorbed light show the inverse trend compared to that for transmitted light. The absorbed TE light is significant higher than the TM light. This effect is independent on the duty cycle and resulting different mask transmission (see Figure 8a). Since the polarization effect increases when going to smaller pitch sizes, the ratio between absorbed TE and TM light also changes. 1:1 AttPSM grating structures inducing a stronger absorption of TE light (see Figure 8b), especially when the pitch size is smaller than 360nm. This behavior results in different energy absorption for grating structures having different pitch sizes and different orientations to the light polarization direction.

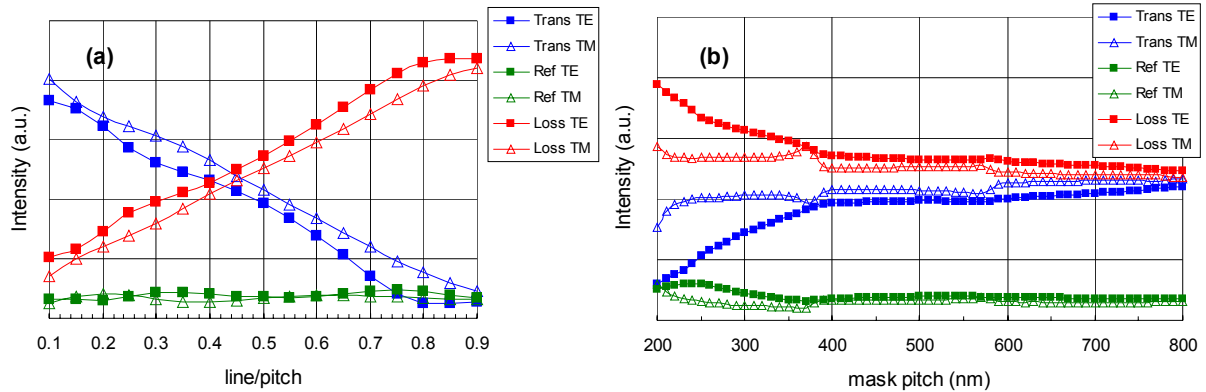


Figure 8: Simulated energy distributions of transmitted (Trans), reflected (Ref) and absorbed (Loss) light of an attenuated PSM for different duty cycles (on the left side) and for varying half pitch sizes (on wafer scale).

5. POLARIZATION MEASUREMENTS RESULTS and DISCUSSION

5.1. Polarization Measurements of Attenuated Phase-Shift Masks

Figure 9 and Figure 10 show the transmission of dense lines-and-space gratings of the attenuated PSM for various pitch sizes and constant duty cycle (line/space=0.5) for two different illumination settings: normal incidence and 20° off-axis illumination. All simulated transmission curves qualitatively reproduce the trend of the experimental data points. The measurements at normal incidence exhibit a pronounced scattering, whereas this effect is reduced for measurements at off-axis illumination. This measurement error could be caused by the back-reflections of the mask in the measurement system (see Figure 4). Furthermore an offset between the simulations curves and measurement points could be observed, e.g. the measured transmission is lower than the simulated transmission. This behavior is more pronounced for the transmission measurement of the 0th diffraction order, when using TM light.

In the case of measuring the transmission of the 0th diffraction order (see Figure 9a), the intensity of TM light is higher compared to that of TE light in the whole mask pitch range. The offset between TE and TM intensity is increasing when decreasing the pitch size. In the other case of measuring the -1st order, the observed transmission of TE and TM light is approximately the same for pitch sizes greater than 400nm (see Figure 9b). For smaller mask pitches the TE transmission suddenly falls down, whereas the TM light transmission remains nearly constant. The TE transmission drop in the first order shifts to smaller pitch sizes, when going to off-axis illumination (see Figure 10b).

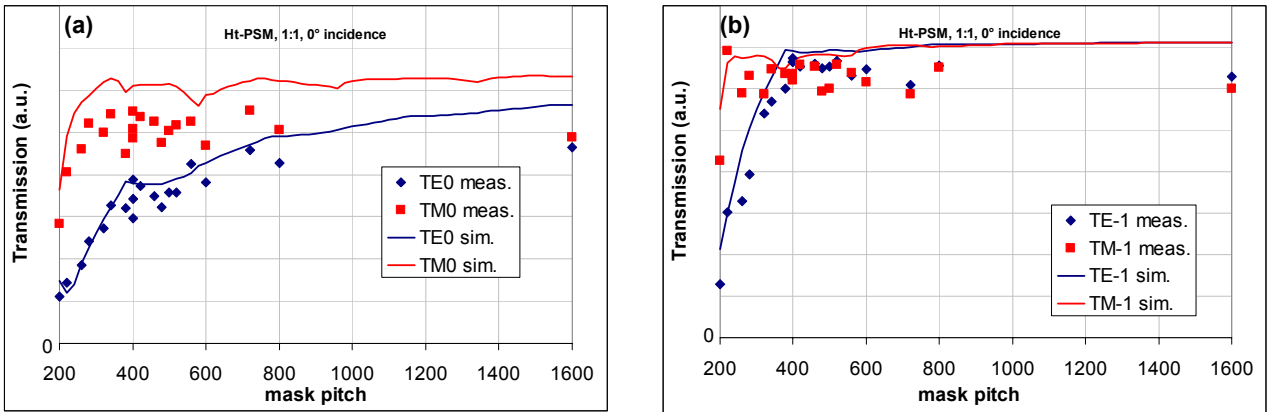


Figure 9: Comparison between measured (squares) and simulated (line) normalized transmission intensities of 0th (a) and -1st (b) diffraction order of illuminated dense lines /space gratings with constant duty cycle (line/space=0.5) and varying pitch size under normal incidence.

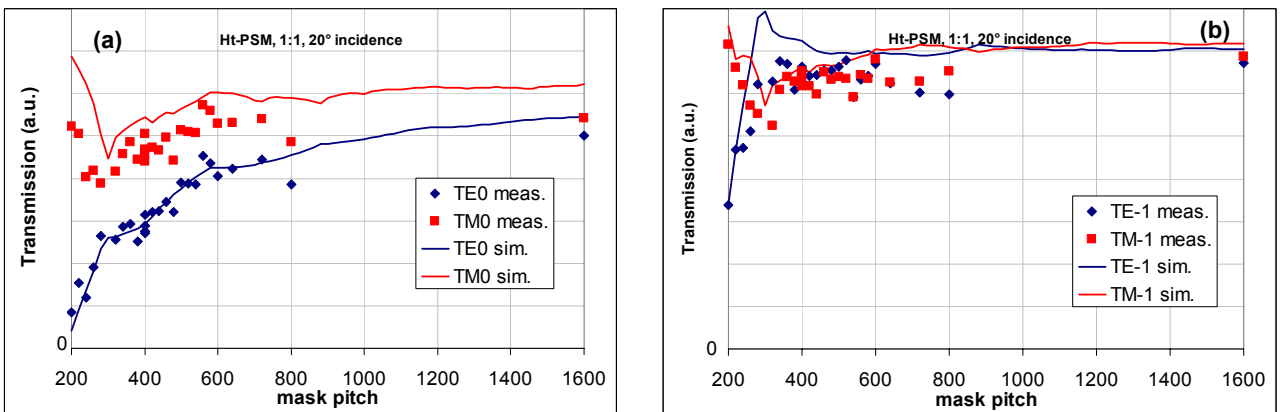


Figure 10: Comparison between measured (squares) and simulated (line) normalized transmission intensities of 0th (a) and -1st (b) diffraction order of illuminated dense lines /space gratings with constant duty cycle (line/space=0.5) and varying pitch size under off-axis illumination (20°).

The measured transmission data were used to derive the degree of polarization (see Equation 3). The resulting DoP-curves are shown on Figure 11 for different illumination angles. A good agreement between measurement and simulation has been observed, although a slight offset for the DoP of the -1^{st} diffraction order is visible. In both illumination cases the DoP of the 0^{th} order is negative within the whole measured pitch range (200-1600nm), e.g. it shows a TM polarization. Furthermore the above-described Wood's Anomalies that appear as discontinuities at 380nm and 580nm were also being resolved in the measurements curve. The DoP of the -1^{st} diffraction order shows a different behavior: the polarization is relatively small in the pitch range 400nm-1600nm, for pitches smaller than 400nm the DoP curve point out a sudden decrease in the case of normal incidence indicating a TM polarization. In the case of 20° off-axis illumination the measurement curve shows a pronounced peak in the TE domain but for pitches smaller than 250nm a TM polarization.

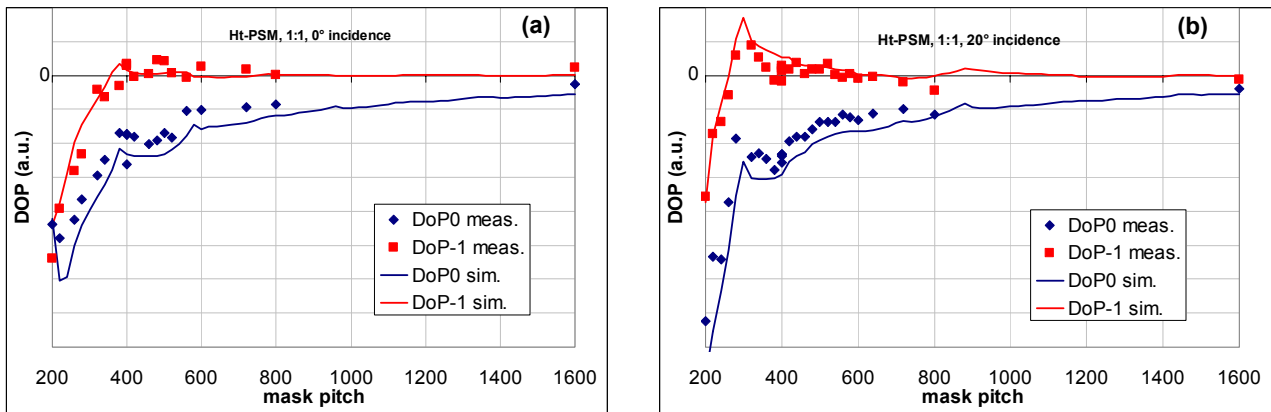


Figure 11: Comparison of measured (squares) and simulated (line) degree of polarization (DoP) of 0^{th} and -1^{st} diffraction orders of illuminated dense lines /space gratings with fixed duty cycle (line/space=0.5) and varying pitch size under normal incidence and 20° off-axis illumination.

The transmission of attenuated PSM gratings with fixed pitch size (400nm) and varying duty cycle (line/space = 0.1-0.6), corresponding to a wafer half pitch of 50nm, was investigated in another series of experiments. The transmission from simulation and measurements were compared and illustrated in Figure 12 and in Figure 13. A good agreement can also be observed, although the measurement points are fluctuating significantly. The resulting polarization degree curves are shown in Figure 14 for normal incidence and off-axis illumination. A significant difference in the degree of polarization can be observed. Whereas the light of the 0^{th} order is in the whole duty cycle range partially TM polarized, the light of the -1^{st} order is mainly partially TE polarized. The DoP of both diffraction orders depends slightly on the duty cycle as well as on the angle of incidence.

Summarizing the results on attenuated phase-shifting masks, the mask-induced partial polarization could be observed as a significant effect, when illuminating dense lines/space structures. The DoP depends strongly on the grating pitch. A strong increase of the polarization has been observed for pitches smaller than 400nm. Under the investigated illumination settings the 0^{th} order is always TM-polarized, whereas the -1^{st} could be both TE and TM polarized, depending on pitch and duty cycle.

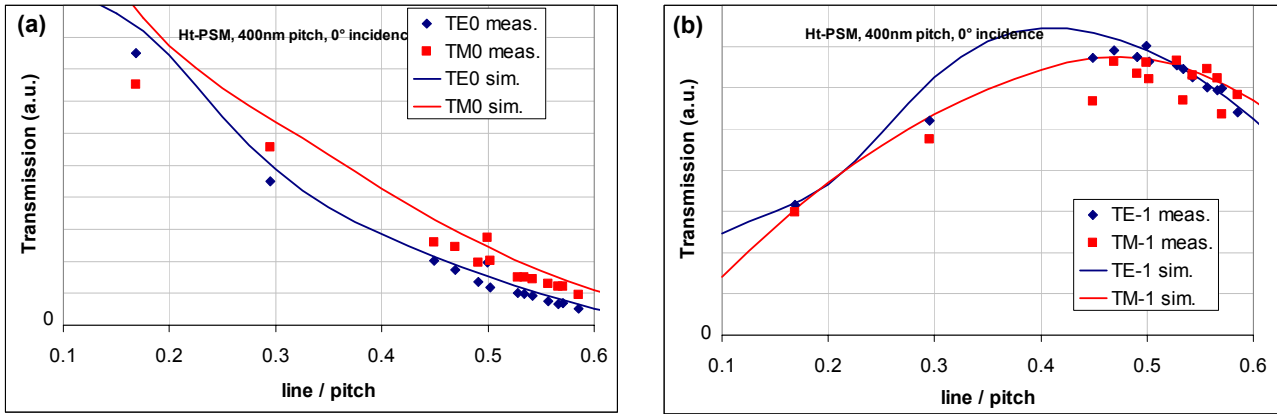


Figure 12: Comparison between measured (squares) and simulated (line) normalized transmission intensities of 0th (left) and -1st (right) diffraction order of illuminated dense lines/space gratings with varying duty cycle and constant pitch size (400nm) under normal incidence.

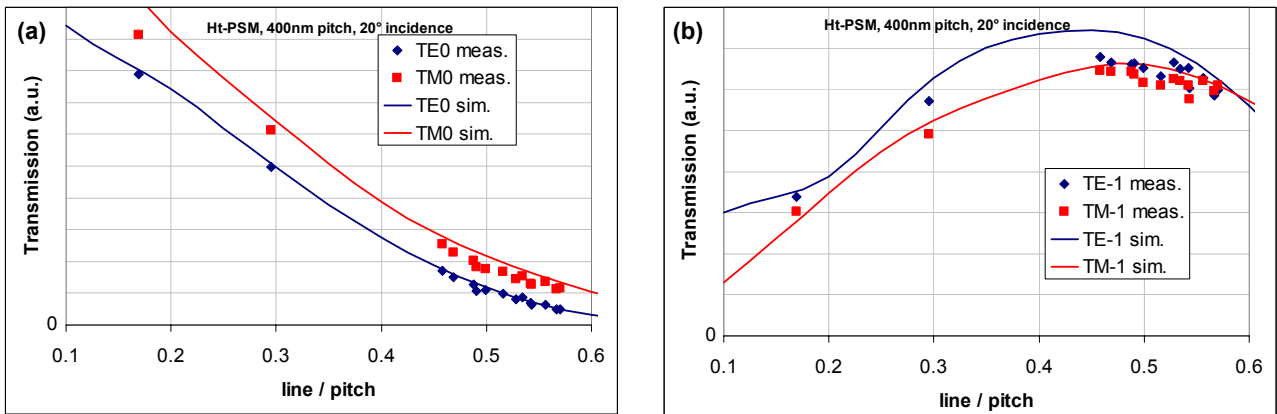


Figure 13: Comparison between measured (squares) and simulated (line) normalized transmission intensities of 0th (left) and -1st (right) diffraction order of illuminated dense lines/space gratings with varying duty cycle and constant pitch size (400nm) under off-axis illumination (20°).

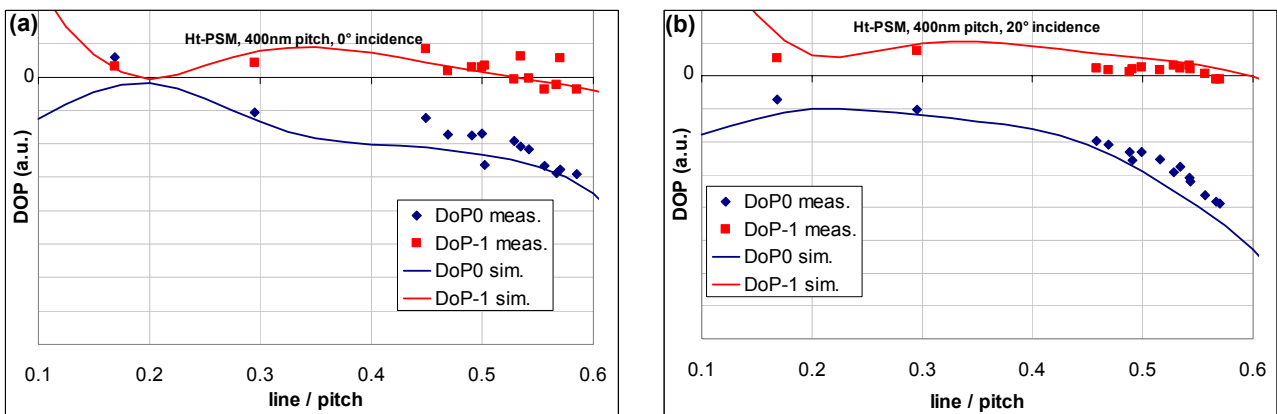


Figure 14: Comparison between measured (squares) and simulated (line) degree of polarization (DoP) of 0th and -1st diffraction orders of illuminated dense lines/space gratings with varying duty cycle and constant pitch size (400nm) under normal (left) and off-axis illumination (20°).

5.2. Polarization Measurements of Binary Masks

A binary mask with comparable dense lines/and space structures was investigated in a second experiment. The same transmission measurements were performed in order to determine the polarization properties of those binary mask-grating structures. The main results are illustrated in Figure 15 and in Figure 16. A general offset between the measurements and simulation results was observed that is significantly higher than for the measurements on AttPSM structures. Several causes could explain such a difference. First of all, the DoP of the binary mask structures is much smaller compared to that of the AttPSM, resulting in a stronger measurement error for the DoP. Furthermore, in the simulation a 2-layer model was used that reflects the optical properties of the chromium-based absorber layer. This n&k model does not correctly reflect the reality, as the absorber layer is not a simple 2-layer system, but rather a graded film. Both effects are reflected in the deviation between simulation and experiment.

Nevertheless, one can observe that in the case of illumination under normal incidence of 1:1 grating structures the DoP of the 0th diffraction order is rather small and mainly negative, indicating partial TM polarization. The DoP of the -1st order is also relatively small, but show a peak at pitch size ~360nm, resulting in partial TE polarization. This peak is more pronounced reaching a higher maximum when setting the illuminating to 20° incidence.

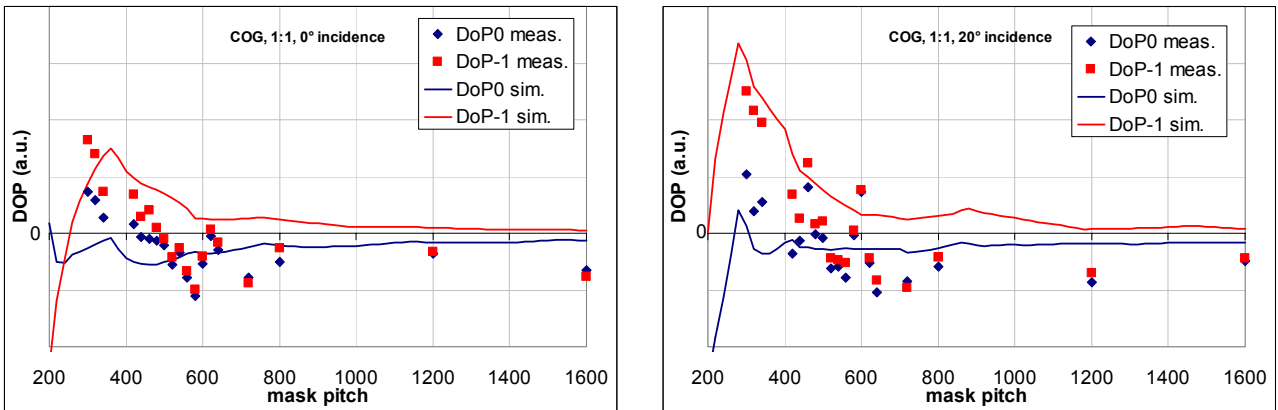


Figure 15: Comparison between measured (squares) and simulated (line) degree of polarization (DoP) of 0th and -1st diffraction orders of illuminated dense lines /space gratings with constant duty cycle (line/space=0.5) and varying pitch size under normal (left) and off-axis illumination (20°).

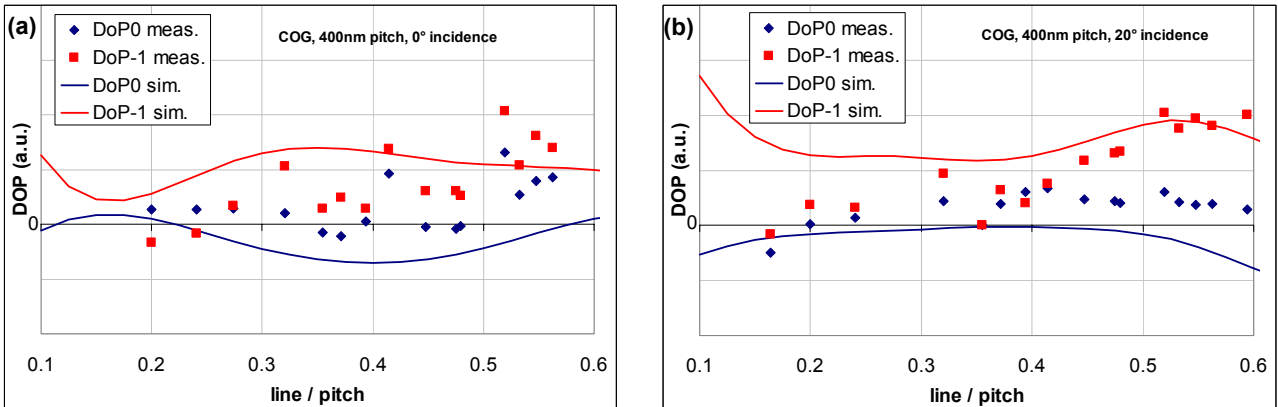


Figure 16: Degree of polarization (DoP) of 0th and -1st diffraction orders of illuminated dense lines /space gratings with varying duty cycle and fixed pitch size (400nm) under normal (left) and off-axis illumination (20°): comparison between measurement (squares) and simulation (line).

The simulated and measured DoP for constant pitch and varying duty cycle is shown in Figure 16. The measured DoP points are in the positive and negative range and only in positive range for 0th and -1st order, respectively. Although there is qualitative agreement between measurement and simulation, a significant offset to simulation and a scattering of the measurement points is visible. No dependence of the DoP on the incidence angle was observed.

In summary, binary masks induce relatively small polarization compared to their phase shifting counterpart. The chromium-based material shows partial TE polarization in first order and very small polarization in 0th order, whereas the molybdenum-silicon-based material reveals a smaller TE polarization in -1st order and a stronger TM polarization in 0th order. The DoP of binary masks depends also on the grating pitch and on the incidence angle.

5.3. Influence of Mask Properties on Polarization Simulation

Further simulation was performed to evaluate the influence of the mask geometry on polarization. As described in section 2, the manufacturing process of attenuated phase-shifting masks could lead to a variation of the trench depth in the quartz as well as to a variation of the sidewall angle. The simulation results of both cases are illustrated in Figure 17 and Figure 18 for 1:1 structures with varying the mask pitch size. Figure 17 and Figure 18 suggest that both effects have a minor influence on the polarization degree. In the simulated cases the DoP deviation is mainly smaller than 2%. Only for pitch sizes <300nm an increased etch depth results in a DoP deviation of up to 8%.

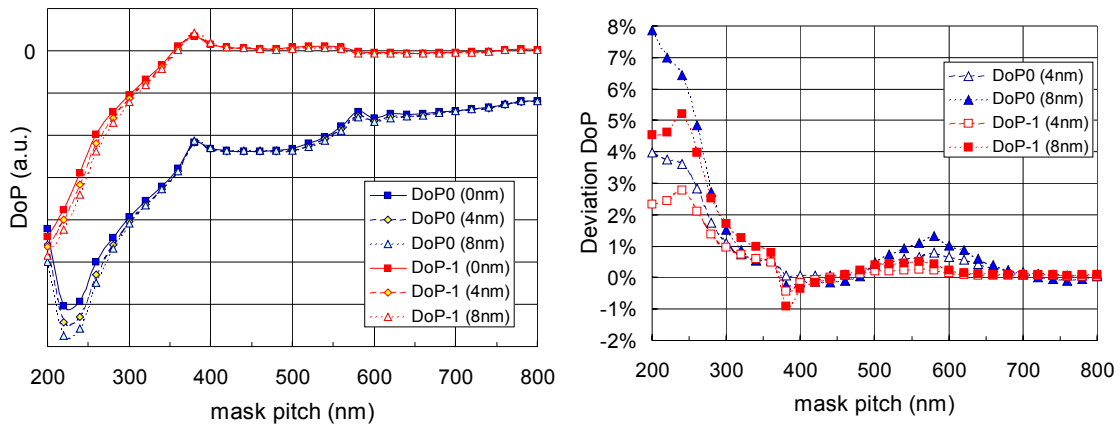


Figure 17: Left: Simulated DoP of 1:1 Att-PSM gratings having different quartz etch depths (0, 4, 8nm); Right: DoP deviation of grating structures with quartz trenches compared to those without trenches.

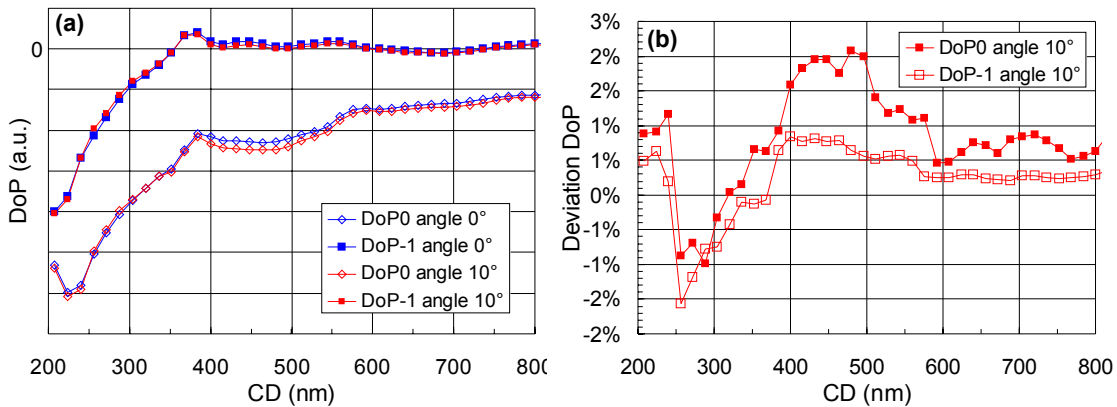


Figure 18: Left: Simulated DoP of 1:1 Att-PSM gratings having different sidewall angles (0°, 10°); Right: DoP deviation of structure with nonzero sidewall angle compared to those with vertical structures.

6. CONCLUSION

Mask induced polarization effects were investigated with standard lithographic masks, which become important at small feature sizes, especially for future technology nodes smaller 45nm half pitch (on wafer scale). A halftone phase shift mask and a binary mask with dense lines/space grating structures were produced. Both masks were used measuring the transmission of the 0th and -1st diffraction order. The mask induced polarization degree was derived from these measurements. The measurement results show a strong dependence on the mask features sizes, especially on the pitch size, on the duty cycle as well as on the absorber material. In general, the polarization effects become important for mask features smaller than 360nm pitch size, corresponding to 45nm wafer half pitch. Furthermore, the measured polarization degree of binary masks is smaller compared to halftone phase shift masks. Whereas binary mask show mainly small partial TE polarization, AttPSM masks induce mainly TM polarization.

Simulations on mask polarization effects were also performed to check the measurement results. In the case of AttPSM both measurements and simulation results show a good agreement, although the measurements show a scattering coming from measurement errors. This leads to a conclusion, that the theoretical description of optical properties of the mask layer stack agrees well with the real mask properties. In the case of binary mask the situation is a bit different. A qualitative good agreement between measurement and simulation was also observed, but in comparison a more pronounced scattering of the measurement points as well as a significant offset between both were seen. Two reasons could be the source of that discrepancy. At first the theoretical model of the simulations does not describe the real optical mask properties well, secondly the measurement error is more significant compared to the relatively small DoP numbers. More investigation is required to understand this issue.

In order to evaluate the influence of the mask induced polarization effect on the imaging performance for the 50nm structures (half pitch wafer scale) first simulations have been performed. The results suggest, that the mask polarization effect of standard 193nm mask materials could be used for the immersion lithography on 50nm structures [4].

REFERENCES

1. A. Estroff, Y. Fan, A. Bourov, F. Cropanese, N. Lafferty, L. Zavyalova and B. Smith, *Mask induced Polarization*, SPIE2004.
2. J. Heber, A. Gatto, N. Kaiser, *Spectrophotometry in the vacuum UV*, Boulder 2002.
3. Web site reference: <http://www.gsolver.com/>
4. K. Bubke, S. Teuber, I. Hoellein, H. Becker, H. Seitz, U. Buttgerit, *Investigation of Polarization Effects on new Mask Materials*, t.b.p. in SPIE 2005
5. A. Erdmann, *Mask Modeling in the Low k_1 and Ultrahigh NA Regime: Phase and polarization effects*, t.b.p.

ACKNOWLEDGEMENTS

The authors would like to thank the Fraunhofer Institute IOF in Jena for their measurement capability and also for a lot of fruitful discussions. Furthermore we would like to thank AMD and IFX for their support on this project. This research was supported by the German Federal Ministry of Education and Research (BMBF) under contract No. 01M3154A (“Abbildungsmethodiken für nanoelektrische Bauelemente”).